



**HAL**  
open science

## A proteomic and cellular analysis of uropods in the pathogen *Entamoeba histolytica*.

Jacques Marquay Markiewicz, Sylvie Syan, Chung-Chau Hon, Christian Weber, Daniela Faust, Nancy Guillen

► **To cite this version:**

Jacques Marquay Markiewicz, Sylvie Syan, Chung-Chau Hon, Christian Weber, Daniela Faust, et al.. A proteomic and cellular analysis of uropods in the pathogen *Entamoeba histolytica*.. PLoS Neglected Tropical Diseases, 2011, 5 (4), pp.e1002. 10.1371/journal.pntd.0001002 . inserm-00691403

**HAL Id: inserm-00691403**

**<https://inserm.hal.science/inserm-00691403>**

Submitted on 26 Apr 2012

**HAL** is a multi-disciplinary open access archive for the deposit and dissemination of scientific research documents, whether they are published or not. The documents may come from teaching and research institutions in France or abroad, or from public or private research centers.

L'archive ouverte pluridisciplinaire **HAL**, est destinée au dépôt et à la diffusion de documents scientifiques de niveau recherche, publiés ou non, émanant des établissements d'enseignement et de recherche français ou étrangers, des laboratoires publics ou privés.

# A Proteomic and Cellular Analysis of Uropods in the Pathogen *Entamoeba histolytica*

Jacques Marquay Markiewicz<sup>1,2</sup>, Sylvie Syan<sup>1,2</sup>, Chung-Chau Hon<sup>1,2</sup>, Christian Weber<sup>1,2</sup>, Daniela Faust<sup>1,2</sup>, Nancy Guillen<sup>1,2\*</sup>

**1** Institut Pasteur, Unité Biologie Cellulaire du Parasitisme, Paris, France, **2** INSERM U786, Paris, France

## Abstract

Exposure of *Entamoeba histolytica* to specific ligands induces cell polarization via the activation of signalling pathways and cytoskeletal elements. The process leads to formation of a protruding pseudopod at the front of the cell and a retracting uropod at the rear. In the present study, we show that the uropod forms during the exposure of trophozoites to serum isolated from humans suffering of amoebiasis. To investigate uropod assembly, we used LC-MS/MS technology to identify protein components in isolated uropod fractions. The galactose/N-acetylgalactosamine lectin, the immunodominant antigen M17 (which is specifically recognized by serum from amoeba-infected persons) and a few other cells adhesion-related molecules were primarily involved. Actin-rich cytoskeleton components, GTPases from the Rac and Rab families, filamin,  $\alpha$ -actinin and a newly identified ezrin-moesin-radixin protein were the main factors found to potentially interact with capped receptors. A set of specific cysteine proteases and a serine protease were enriched in isolated uropod fractions. However, biological assays indicated that cysteine proteases are not involved in uropod formation in *E. histolytica*, a fact in contrast to the situation in human motile immune cells. The surface proteins identified here are testable biomarkers which may be either recognized by the immune system and/or released into the circulation during amoebiasis.

**Citation:** Marquay Markiewicz J, Syan S, Hon C-C, Weber C, Faust D, et al. (2011) A Proteomic and Cellular Analysis of Uropods in the Pathogen *Entamoeba histolytica*. PLoS Negl Trop Dis 5(4): e1002. doi:10.1371/journal.pntd.0001002

**Editor:** Anuradha Lohia, Bose Institute, India

**Received:** August 18, 2010; **Accepted:** March 7, 2011; **Published:** April 5, 2011

**Copyright:** © 2011 Marquay Markiewicz et al. This is an open-access article distributed under the terms of the Creative Commons Attribution License, which permits unrestricted use, distribution, and reproduction in any medium, provided the original author and source are credited.

**Funding:** This work was funded by an INCO-DEV grant as part of the EU Fifth RTD Framework Programme and was supported by a grant from the Pasteur-Weizmann Research Council and by a grant from ARN-MIE8 to NG. The funders had no role in study design, data collection and analysis, decision to publish, or preparation of the manuscript.

**Competing Interests:** The authors have declared that no competing interests exist.

\* E-mail: nguillen@pasteur.fr

## Introduction

The acquisition of cell polarity is a crucial requirement for motility in a variety of cells, including activated leukocytes and fast-moving amoebae. Cell polarization is defined by the presence of an anterioposterior cell axis and two functionally and morphologically distinct poles: the leading edge, which guides the cell's directional movements, and the trailing edge (i.e. the uropod), which accumulates adhesion molecules. Following surface receptor activation and subsequent patching and capping, uropods form concomitantly with a retrograde flow of the cortical actomyosin cytoskeleton. It has been suggested that these dynamic properties are closely related to how cells move [1,2]. However, an important body of evidence indicates that uropods are essential for other relevant cell functions, such as cell-cell communication and cell adhesion. Uropods are found in neutrophils, monocytes, natural killer cells and amoebae and appear to have an important role in immune-related interactions [3]. For instance, adhesion molecules are recruited into cellular uropods following exposure to chemokines. This process constitutes an important step in the mechanism responsible for the recruitment of leukocytes to the inflammation site. Although these phenomena are involved in immune responses during inflammation (in the case of leukocytes) or infection (in the case of amoebic parasites), the interplay between uropod formation and surface receptor capping is still poorly characterized.

Human amoebiasis is a persistent, infectious disease whose symptoms vary from amoebic colitis with destruction of the intestinal epithelium and severe dysentery to extra-intestinal abscesses particularly in the liver [4,5]. In amoebiasis, the parasite *Entamoeba histolytica* employs a range of diverse strategies for immune evasion. The most distinctive strategy is surface receptor capping, in which surface targets for host immune components are translocated towards the uropod and then released into the culture medium [6,7]. This membrane shedding also enables *E. histolytica* to discard bound, harmful substances such as anti-amoeba antibodies and complement. Surface receptors circulate between the cell surface and the intracellular compartment via internalization in active endocytic processes. The residence time of these surface receptors in the endocytic compartment depends on the receptors' functions. The fact that uropods are discarded from the cells (thus reducing the extent of endocytosis) suggests that (i) the isolated fraction concentrates various molecules to the plasma membrane and (ii) the excreted molecules are likely to have a relevant effect on the establishment of amoebiasis. Therefore it is essential to identify the major components of discarded fractions to understand the mechanism of uropod formation.

During invasive amoebiasis, *E. histolytica* attaches to its target cell via the galactose/N-acetylgalactosamine lectin (Gal/GalNAc) and performs contact-dependent cell killing [8]. Although the main target cell-binding protein Gal/GalNAc is not exclusively expressed at the cell surface, it is an immunodominant molecule

## Author Summary

Uropods are membrane folds formed at the rear of moving cells, e.g. lymphocytes during immune responses and the amoebic parasite *Entamoeba histolytica* during amoebiasis. Previous studies showed some surface receptors of *E. histolytica*, e.g. the Gal/GalNAc lectin, which is involved in adhesion, undergo capping and accumulate at the uropod, and these processes are driven by the activities of the actin-rich cytoskeleton. These uropods are then discarded to the extracellular medium, suggesting the components of uropods may induce anti-amoebic responses from the host. In this study, we showed that the serum from patients infected with *E. histolytica*, but not serum from healthy individuals, is able to induce uropod formation. To characterize the proteome of these induced uropods, we performed a proteomic analysis of the discarded complexes. In addition to the presence of several proteases and novel cytoskeleton factors, our proteomic results highlight the presence of important surface components including the Gal/GalNAc lectin, calreticulin, several adhesion molecules and the immunodominant antigen M17. Finally, we derived two important conclusions from further cellular analyses. Firstly, cysteine proteases are not involved in uropod formation in *E. histolytica*. Secondly, M17 was confirmed to be recruited at the uropods induced by serum from infected patients.

which can induce IgA antibody secretion in amoebiasis patients [9]. The Gal/GalNAc lectin is composed of two subunits: a 170 kDa heavy chain (HgL) with a transmembrane domain and a cytoplasmic tail with motifs sheared with the signalling molecule  $\beta 2$  integrin (an integrin receptor subunit involved in cell-cell adhesion) [10], and a 30/35 kDa light chain (LgL). The LgL subunit is attached to the membrane by a GPI anchor and to the heavy chain via disulfide bonds. The complex is associated with the 120-kDa intermediate subunit (IgI) [11,12], which also contains a GPI anchor. When *E. histolytica* is incubated in the presence of lectins such as concanavalin A (Con A, which has been widely used to investigate receptor capping), the Gal/GalNAc lectin accumulates at the uropod [13,14,15]. Remarkably, blocking out-to-in signalling by using a dominant negative strategy against the HgL subunit [10,15] leads to a reduction in parasite adhesion to cells and in Gal/GalNAc lectin clustering of receptors by Con A. The HgL dominant negative parasites are unable to move and thus impact pathogenesis since these do not produce effective liver infection in the hamster model of hepatic amoebiasis [16,17]. However, these amoeba are still able to invade the human colon effectively in an experimental model of intestinal amoebiasis [18]. Interaction between the HgL carboxyl-terminal domain and the amoebic cytoskeleton (via actin-binding proteins such as  $\alpha$ -actinin) [19] is a key step in this signalling pathway and determines the tissue specificity of Gal/GalNAc lectin. Recently, the light chains have also been found to be important for Gal/GalNAc lectin capping activity, since the absence of LgL subunits 1 to 3 affects the parasites' ability to cap and translocate the Gal/GalNAc lectin to the uropod region [20]. Insight into the capping process's mechanism has also been gained recently: a serine protease from the rhomboid family concentrates in the vicinity of the uropod and cleaves the Gal/GalNAc HgL subunit *in vitro* [21]. These findings highlight the potential role of a large number of amoebic proteases in surface receptor capping and uropod formation. Functional links between proteinases and uropod formation have also been observed in other eukaryotic cells. For instance, leukocyte migration is promoted by the activity of

cathepsin X, a cysteine peptidase localized at the uropod and which modulates the interaction between  $\beta 2$  integrin and the actin-rich cytoskeleton [22,23]. In addition to the Gal/GalNAc lectin, calreticulin (CRT) was found to be another antigen localized in the uropod in addition to its localization in the endoplasmic reticulum [24]. CRT has an important role in a variety of cellular processes, including Calcium signalling and protein folding. The fact that CRT is an immunodominant antigen during hepatic amoebiasis [25] suggests that it may be involved in the onset of inflammation and the immune response.

Receptor capping at the amoebic surface and then extrusion of uropod fractions both require active remodelling of the actomyosin cytoskeleton [13,26]. These cytoskeleton functions are regulated by a panel of important proteins, including the small GTPases RacG [27] and RacA [28], their corresponding GTP exchange factors [29,30,31], the PAK kinases [32,33] and the actin-filament cross-linker Filamin A (previously referred to as ABP120) [34]. Blocking myosin II inhibits surface receptor capping and, as a result, trophozoites are unable to invade living tissues [15].

To gain insight into the molecular composition of uropods, we performed a high-throughput LC-MS/MS proteomic analysis of the uropod-extruded fraction following incubation of *E. histolytica* with Con A. Our results confirmed the expected presence of the Gal/GalNAc lectin and CRT. In addition, our results also suggest the presence of immunodominant variable surface antigen M17 [35], a number of proteins involved in multiple drug resistance [36], a set of specific ATPases, a number of small GTPases, cysteine proteases, at the uropod enriched fractions. Given the potential roles of immunodominant M17 antigen and cysteine proteases in the pathogenesis of amoebiasis, we verified the enrichment of M17 at uropod and investigated the potential roles cysteine proteases in uropod formation, using cell biology approaches. To the best of our knowledge, this is the first report on the uropod proteome in any cell. The *E. histolytica* surface proteins identified in this study may provide new insights into the biology of the parasite. Indeed, the uropod components appear to be testable biomarkers which may be either recognized by the immune system and/or released into the blood. The molecular and cellular analysis of uropod extruded fractions thus opens up opportunities for better understanding the mechanism of amoebic infection.

## Methods

### Parasite culture and cysteine protease inhibition

The pathogenic *Entamoeba histolytica* (wild type, HM1: IMSS strain) was cultured axenically in TYI-S-33 medium [37] at 37°C. For protease inhibition tests,  $1.8 \times 10^5$  trophozoites in 1.5 ml of TYI-S-33 medium were incubated for 3 h at 37°C in the presence of (2S, 3S)-trans-Epoxy succinyl-L-leucylamido-3-methylbutane (E-64c, Sigma) or (2S, 3S)-trans-Epoxy succinyl-L-leucylamido-3-methylbutane ethyl ester (E-64d, Sigma) [38]. 100  $\mu$ M of both E64 were used, at this concentration the enzymatic activity of cysteine proteases is inhibited by 95% as measured by the degradation of the synthetic substrate Z-RR-AMC (Sigma) (data not shown). Then the parasites were washed in PBS twice, resuspended in 1 ml of PBS and incubated in the presence of Con A (20  $\mu$ g/ml) as described below.

### Imaging of live *E. histolytica*

For video microscopy, the parasites ( $10^5$  per ml) in PBS were seeded on glass bottom culture dishes (MatTeck) and incubated at 37°C in the presence of 5  $\mu$ g/ml of fluorescent Con A (Alexa fluor

488, Molecular Probes). Live parasites undergoing capping were imaged using a confocal microscope (40× objective) with a Nipkow disk device (Perkin Elmer). Images (10 per second) were processed with ImageJ software (<http://rsb.info.nih.gov/ij>).

### Induction of receptor capping and purification of uropod extruded fractions

*Amoeba* trophozoites ( $5 \times 10^8$ ) were incubated in the presence of Con A (20 µg/ml) (grade VI; Sigma) at 4°C for 1 h. To induce cap formation and release, the cells were moved to 37°C for 10 min and then harvested. The protein fractions were extracted and treated in accordance with previously published methods [13]. Briefly, trophozoites and cellular debris were eliminated by two successive centrifugations at  $300 \times g$  for 5 min. Caps were pelleted at  $30,000 \times g$  for 30 min at 4°C. The final pellet was resuspended and washed twice in 100 ml of PBS containing 1 M  $\alpha$ -methyl-D-mannopyranoside and protease inhibitors (2 mM AEBSF, 1 mM NEM, and 2 mM PHMB). Lipids were removed by washing the pellet in methanol (600 µl), chloroform (150 µl), water (450 µl) and centrifugation at 1000 g for 5 min. The aqueous phase was treated with methanol (450 µl), centrifuged at 1000 g for 5 min and the pellet was dried. The protein fraction and crude extract from growing trophozoites (10 µg) were analyzed by western blot with an anti-Gal/GalNAc lectin antibody prepared in our laboratory [14] against the tail domain of HGL subunit (dilution 1:400) and with an anti-ConA antibody (Sigma) diluted 1:500. Detection was performed with a secondary anti-rabbit antibody and enhanced chemoluminescence.

### Protein analysis by liquid chromatography and tandem mass spectrometry (LC-MS/MS)

Two independent experiments were performed. The dried protein pellet (100 µg, obtained from  $10^8$  cells) was dissolved in 20 µl of 1% SDS and then slowly diluted with 50 mM ammonium bicarbonate to a final concentration of 0.1% SDS. The sample was reduced with DTT and alkylated with iodoacetamide before digestion with 1 µg of modified trypsin (Promega) for 24 hrs at RT. A second 1 µg of trypsin was added and digestion was allowed to proceed for an additional 24 hrs. The sample was then desalted and ion-exchanged before concentration. Around 30% of the digest was introduced into the mass spectrometer for analysis. Two runs (technical replicates) were performed using slightly different instrument data acquisition parameters, so that as many different proteins as possible could be identified. The full LC-MS/MS procedure was performed by the Biomolecular Research Facility at Virginia University (1300 Jefferson Park Avenue, Jordan Hall, Room 1101, Charlottesville, VA 22908, USSA, tel. +1 434 924-2356). The LC-MS system consisted of a Finnigan LTQ-FT ion trap - ion cyclotron resonance mass spectrometer system with a Protana nanospray ion source, interfaced to a self-packed 8 cm × 75 mm id Phenomenex Jupiter 10 mm C18 reversed-phase capillary column. 0.5–10 µl volumes of the extract were injected and the peptides were eluted from the column by an acetonitrile/0.1 M acetic acid gradient at a flow rate of 0.25 µl/min. The nanospray ion source was operated at 2.8 kV. The digest was analyzed using the instrument's double-play capability by acquiring (i) full scan mass spectra to determine peptide molecular weights and (ii) product ion spectra to determine the amino acid sequence in sequential scans. This mode of analysis produces approximately 10,000 collisionally-activated dissociation (CAD) spectra of ions ranging in abundance over several orders of magnitude. Not all CAD spectra were derived from peptides. The data were processed using Sequist in the Thermo Electron

Bioworks program ver 3.3.1 (instrument software Xcalibur 2.0) against the *E. histolytica* proteome downloaded from NCBI (genome version 2005). Parent mass tolerance of 8 ppm, fragment ion tolerance of 0.8 Da. The Xcorr scores adopted the following thresholds: +1 > 1.8, +2 > 2.2, +3 > 2.7, +4 (and higher) > 3.5. The search included CAM Cys as a static modification and Ox Met as a differential modification. Then Scaffold version 3\_00\_03 computer program was then used to analyse the data (569 proteins were identified with 0.2% of FDR). Then identity of proteins was further confirmed in the *E. histolytica* reannotated genome (Pathema, data version 5.0). The complete data set was deposited to Tranche database (<https://proteomecommons.org/tranche/>). The accession number of the dataset, which is called "hash", is: C94k72mNyTtP6PDjuFbpsRJuviEokUNGt6joLkg-wIJuSNl5SYz/iruupzJPKc1CZabar3up98e2syGVm/g75qEjnV-QAAAAAAAAAB3g == .

### Immunofluorescence staining and confocal microscopy

Trophozoites ( $2 \times 10^6$ /ml) were incubated in PBS containing fluorescent Con A (5 µg/ml) and non-fluorescent Con A (10 µg/ml) or human serum (40 µl/ml) for 5 min at 37°C. Naive human serum ( $n = 3$ ) was obtained through the Pasteur Institute's DIAGMICOLL project (registration n° RBM #816) and sera from patients ( $n = 2$ ) were a gift from Dr M. C. Rigotherier (Faculty of Pharmacy Châtenay-Malabry, France). Three experiments were conducted. The parasites were fixed in 3.7% formaldehyde for 30 min and incubated in 50 mM  $\text{NH}_4\text{Cl}$ /PBS for 30 min. In some cases, cells were permeabilized by adding 0.1% Triton  $\times 100$  for 1 min and the samples were then blocked in 1% BSA/PBS for 30 min at 37°C. Preparations were then incubated with the following antibodies (diluted 1:100) raised in rabbits: anti-M17 (raised against the peptides GTKPKewTMKYTKYP and ENNFESKYSIKRDST in this work), and anti CP-A5 or anti-CP-A1-A2 [39], a kind gift of Dr Tomoyoshi Nozaki (National Institute of Infectious Diseases, Japan). The anti-human or anti-rabbit secondary antibodies coupled to Alexa 488 or Cy3 (Molecular Probes) were added at a dilution of 1:200 for 30 min at 37°C. *Amoeba* were examined by confocal microscopy (microscope LSM510, Zeiss). When necessary the number of uropods was determined in the total fraction of counted parasites summed from the three experiments.

### Substrate gel electrophoresis

1 µg of uropod proteins was migrated on 10% SDS-polyacrylamide gel co-polymerized with 0.1% gelatine (w/v). After removal of SDS by shaking the gel in 2.5% Triton X-100 for 30 min, and subsequent incubation of the gels overnight at 37°C in 0.1 M sodium phosphate buffer pH 6.5, containing 2.5 mM dithiothreitol, gelatinase activity was detected as a clear band in the Coomassie Brilliant Blue-stained gels.

## Results

### Uropod formation and release from *E. histolytica*

To determine the kinetics of uropod formation and release, we imaged live parasites incubated with fluorescent Con A (FITC-Con A). The process was observed by rapid acquisition in confocal laser microscopy using a Nipkow disk device (Video S1 and Figure 1). Initially, Con A bound uniformly to the cell surface and indicated a symmetrical receptor distribution. Activation of receptor capping induced changes in the cell shape and probably accounted for the asymmetrical distribution of the FITC-Con A ligand; the latter was absent from the front of the cell but was concentrated in the uropod (Figure 1A). Internalization of ligand-receptor complexes was

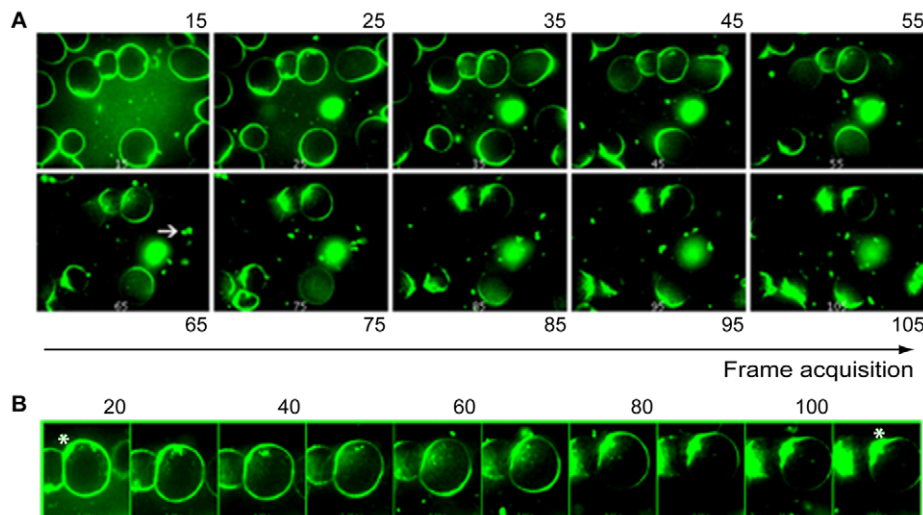


**Figure 1. Spatiotemporal analysis of the redistribution of Con A associated with the surface of *E. histolytica*.** Trophozoites (of 20–30  $\mu\text{m}$  size) were incubated under the microscope at 37°C and fluorescent Con A was added at the starting time point. *In vivo* imaging was performed and the uropod formation process was detected by frames (indicated by numbers) recorded in a confocal microscope with a Nipkow disk device. A: the micrograph represents 100 images recorded as 10 images every second. Note the polarisation of fluorescent Con A over time and the increase in the extrusion of particles into the medium (white arrow). B: Enlarged frames from a chosen cell are presented, with the white star marking the end of the trophozoite at which the uropod is formed. The entire sequence lasted 11 seconds. See Video S1 for visualisation of details in real time. doi:10.1371/journal.pntd.0001002.g001

observed in some cells as intracellular fluorescent spots, indicating the presence of an active endocytic process during receptor capping. The process of uropod formation and release occurred rapidly (in 5 to 10 seconds) (Figure 1B). The extruded fractions accumulated in the medium and were observed as extracellular fluorescent agglomerates.

Previous work had suggested the release of membrane fractions from trophozoites after incubation with serum from patients suffering from hepatic amoebiasis [7]. We analyzed the ability of human serum (from both healthy individuals and *E. histolytica*-infected patients) to induce surface receptor capping and uropod formation. For each serum tested, parasites were fixed and the presence of caps was determined by epifluorescence using an anti-human secondary antibody (Figure 2). Sera from healthy individuals bound weakly to the surface of *E. histolytica*. Small membrane patches were seen in only 8% of cases (46 out of 582 amoebae, counted in three experiments). In contrast, cell binding and efficient uropod formation (52%: 282 out of 542 amoebae, counted in three experiments) was clearly observed when sera from patients presenting liver abscess were used.

#### LC-MS/MS analysis of protein content in uropod extruded fractions

Uropod extruded fractions (UEF) were recovered, treated as indicated in methods section and submitted to western blot analysis in order to identify the heavy chain of the Gal/GalNAc lectin and Con A as a control (Figure 3A). We applied a high-throughput proteomics approach to uropod-extruded fractions and gained insight into the potential mechanism of surface receptor capping and the signal transduction pathways that induces cap formation and release. After capping induction in  $10^8$  cells from two independent experiments, UEF were analyzed by LC-MS/MS and the peptide sequence data were determined (see Methods) with a Xcorr higher than 1.5 and 0,2% of percentage of false discovery (FDR). A list of proteins was generated taking into account for protein identification 99,9% accuracy, among these we analyzed proteins represented at

minimum by two peptides. A set of 269 proteins was established (The entire data files were submitted to Tranche database (<https://proteomecommons.org/tranche/>). Whereas 36 of these were hypothetical proteins with unknown functions, 104 proteins were present in both experiments and could be categorized using both functional GO-term annotations and manual annotation via BLASTP and InterProScan (for protein domain searches) from the EMBL database (Figure 3B and Table S1). Signalling molecules accounted for a significant proportion of the UEF proteome, with the most numerous being small GTPases from the Rho and Rab families. Metabolic enzymes, biogenesis factors and trafficking-related molecules were present in the UEF proteome. These proteins are linked to plasma membrane and to the endocytic process. Surface molecules, cytoskeletal proteins and amoebic proteases were also identified. Lastly, a potential virulence factor (KRiP3) was found in UEF. We further characterized the surface proteins, the cytoskeleton proteins and the proteinases since these categories are potentially involved in the surface receptor capping process and the anti-amoeba immune reactions (Table 1). In addition to the stringency of protein selection, one important criteria allowing us to go further in this analysis was the fact that for example surface antigens such ARIEL [40], kinase receptors abundant family [41] or  $\beta$ -tubulin (nucleus marker) were not present in this proteomic analysis indicating that we have in the analyzed fraction proteins mostly linked to UEF.

#### Amoebic proteins associated with the cell surface and present in the uropod extruded fraction proteome

The Gal/GalNAc lectin protein complex (within which HgL and LgL subunits were identified) and CRT were representative of amoebic surface-related protein as expected (Table 1). The presence of the lectin complex in caps has been observed by the use of a range of molecular and cellular methods [11,15,42]; as well as the presence of CRT [24]. One important surface protein found at the UEF was the 125 kDa immunodominant antigen M17, which is recognized by sera from patients with amoebic liver abscesses [35]. In addition, the surface related proteins

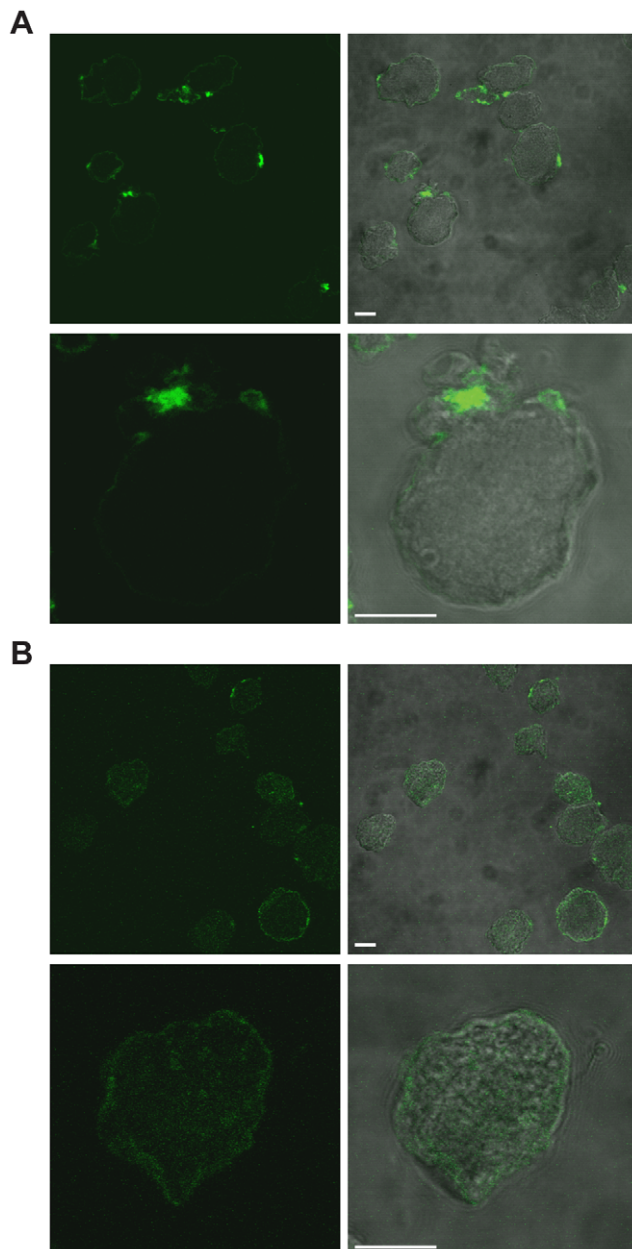


**Figure 2. Serum from amoebiasis patients promotes uropod formation in *E. histolytica*.** The micrographs represent confocal microscopy sections of fixed parasites following incubation with serum from patients with amoebic liver abscesses (A) or from healthy donors (B). The left panels show immunofluorescence images obtained after incubation with anti-human antibodies. The right panels show the overlaid phase contrast/fluorescence images of entire parasites. The detector gain for fluorescence was increased in images shown in panel B. Scale bars: 10  $\mu$ m.

doi:10.1371/journal.pntd.0001002.g002

(EHI\_100320, EHI\_030830, EHI\_016480 and EHI\_074020) contain an ATP-binding cassette from the ABC transporters superfamily. Pgp6 (EHI\_101230) is constitutively expressed in parasites which are resistant to the anti-amoebic drug emetine and is involved in the multiple drug resistance phenotype [36]. We also identified the adhesin ADH112 (EHI\_181220), which is part of a surface and vacuolar heterodimer complex involved in adhesion, cytopathic processes and phagocytosis [43,44]. ADH112 has a cell

adhesion domain at its carboxyl terminal and a Bro-1 signalling domain at its amino terminal [45]. Interestingly, ADH112 shows homology with Alix, a factor that regulates integrin-mediated cell adhesions and extracellular matrix assembly [46]. Another parasite adhesion protein found in the UEF was the serine-, threonine- and isoleucine-rich protein (STIRP). The latter is predicted to be a transmembrane protein encoded by a five member multigene family. It is only present in pathogenic *E. histolytica* [47] and its inactivation reduces parasite adhesion to cultured epithelial cells. Our data indicate that STIRP is a membrane associated component. Lastly, an unknown protein from the CXXC motif-containing family was present. It has a signal peptide and seven furin-like cysteine rich regions that is found in a variety of proteins and involved in signal transduction via receptors tyrosine kinase [48].

### Cytoskeleton-related components present in the uropod extruded fraction proteome

Several proteins linked to the actin-rich cytoskeleton were identified in the UEF proteome (Table 2). Most have already been observed in the uropod region during capping and include actin [15], myosin II heavy chain [13,26], the small GTPase Rac G [27], guanine exchange factors [29], filamin [34] and  $\alpha$ -actinin [19]. Moreover, our proteomic analysis highlighted the signalling pathway leading to surface receptor capping through the discovery of filopodin (EHI\_167130) - an uncharacterized protein with three ezrin/radix/moesin (ERM) domain repeats and one I/LWEQ domain (which binds to actin and is present in talin). Talin has an important role in the interaction between the cytoskeleton and the cell surface receptors [49] and also influences ERM protein function during uropod induction in T lymphocytes [50]. For instance, this is the first report to identify ERM domain-containing protein (which is pivotal for capping of adhesion molecules in lymphocytes) in an evolutionary early branching eukaryote such as *E. histolytica*. This finding suggests an ancient origin for the ERM domain and opens up opportunities for further molecular studies on cytoskeletal activities during receptor capping in *E. histolytica*. The UEF proteome analysis revealed that several actin-binding proteins are related to the spectrin-like protein family (e.g.  $\alpha$ -actinin and filamin). These proteins have already been identified in the *E. histolytica* uropod using cell biology techniques [19,34]. Spectrin family proteins and the associated kinases are known to redistribute to the uropod following T cell activation during the onset of inflammation [51]. The dynamics of actin filaments within the uropod was also illustrated by the presence of factors such as the p41-Arc component of the Arp2/3 complex that is involved in “de novo” actin filament formation [52]. Calcium is one of the most versatile and universal second messengers in cells. It is widely accepted that intracellular Calcium has an effect on the actin cytoskeleton dynamics. Although the calcium-binding proteins of unknown function grainin 1 and grainin 2 were highly abundant in the UEF, a functional link between grainins and the cytoskeleton has not yet been reported in the literature.

### Amoebic proteinases present in the UEF proteome

Proteases were another category of the main factors found in the UEF (Table 2). The cysteine proteases were all endopeptidases (seven in total): CP-A1, CP-A2 and CP-A5 from the very well known A family and CP-C4, C5, -C6 and -C13 from the C family. The C family was recently discovered in *E. histolytica* [53]. Several studies have shown that peptidases (particularly cysteine peptidases) are major pathogenicity factors in *E. histolytica* [54]. CP-A5 is the prime candidate, (although we only found one peptide in experiment I which however covers 5% of the protein), since it

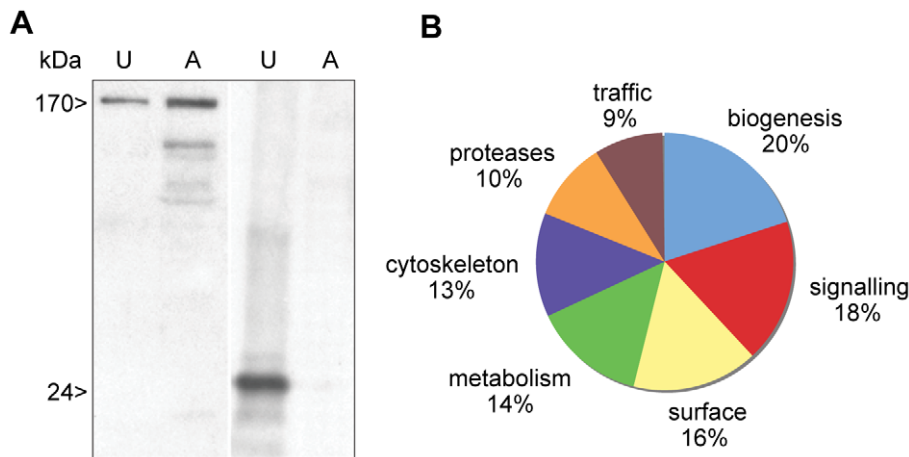


**Figure 3. Distribution in functional categories of the proteins present in the *E. histolytica* uropod extruded fraction.** A. Electrophoretic analysis of proteins from the ConA-uropod complex and from crude extract. A sample of UEF or amoebic extracts (10  $\mu$ g, U = uropod; A = amoebae) were resolved by SDS-PAGE. The Gal/GalNAc lectin heavy chain (170 kDa) and the Con A (24 kDa) were revealed by western blot. B. Protein identification with LC-MS/MS was followed by proteome comparisons using the BLAST computer program, GO annotations and manual annotations. Two LC-MS/MS experiments were performed. Only proteins identified by at least two peptides in each experiment were taken into account. In all, 104 proteins were present in both experiments and could be analyzed. The entire data set was submitted to Tranche (<https://proteomecommons.org/tranche/>) database.

doi:10.1371/journal.pntd.0001002.g003

localizes at the amoebic surface [55] and is involved in human colon invasion [18] and ALA formation [56]. This protease contains an Arg-Gly-Asp (RGD) integrin binding motif which has also been found in the proregion of cathepsin X from higher eukaryotes [57]. In cell-adhesion proteins like fibronectin, RGD motifs serve as ligand recognition sites for cell-surface receptors such as the integrins. Recently, it has been shown that the RGD motif present in the pro-form of amoebic CP-A5 binds to the

integrins of intestinal Caco2 cells and promotes the activation of the NF $\kappa$ B signalling pathway [38]. In addition to cysteine proteinases, we also identified Sp2 one of the members of a family of three amoebic serine proteases (i.e. S28 family) [58] and two dipeptidyl-peptidases from the lipase family which hydrolyze tryglycerides, phospholipids and cholesterol esters [59].

In summary, the present article reports the main features of the proteomic profile obtained by LC-MS/MS analysis of *E. histolytica*

**Table 1. Surface-linked proteins in the uropod extruded fractions.**

Genbank GI	JCVI Accession	Description	Mass (kDa)	Experiment I		Experiment II	
				Unique peptides	% Covery	Unique peptides	% Covery
67479719	EHI_136160	Calreticulin	45	12	29	11	32
67478183	EHI_015380	Immuno-dominant variable surface antigen M17	125	11	10	8	11
405076	N/A	P-glycoprotein 6	143	8	6,9	10	8
183232088	EHI_100320	Multidrug resistance protein	182	8	6,6	9	6,8
183232225	EHI_030830	Plasma membrane calcium-transporting ATPase	114	8	8,5	8	9,2
67475672	EHI_016480	Plasma membrane calcium-transporting ATPase	119	8	4,8	5	4
3392885	N/A	Plasma membrane calcium -transporting ATPase	121	7	6,3	3	3,6
67481663	EHI_012270	Gal/GalNAc lectin heavy subunit	144	6	4,8	7	5
67481591	EHI_035690	Gal/GalNAc lectin light subunit	34	5	2	4	20
67476079	EHI_065670	Cation-transporting P-typeATPase	126	5	2,7	3	3,1
67484480	EHI_148790	Gal/GalNAc lectin light subunit	32	4	17	5	13
305078	N/A	Gal/GalNAc lectin light subunit	34	4	12	2	6
183230108	EHI_012330	Serine-Threonine-Isoleucine Rich Protein	291	4	1,8	2	1
67475812	EHI_074020	Vacuolar proton ATPase subunit	93	3	5,5	7	12
67463605	EHI_111990	CXXC-rich protein	131	3	2	4	3
67474486	EHI_181220	Adhesin 112 (EhADH112)	78	3	5,7	3	8,2
67479029	EHI_095820	ATP-binding cassette transporter MRP	152	3	2,3	3	2,4

doi:10.1371/journal.pntd.0001002.t001

**Table 2.** Cytoskeleton-related and proteinases in UEF.

Genbank GI	JCVI Accession	Description	Mass (kDa)	Experiment I		Experiment II	
				Unique peptides	% Covery	Unique peptides	% Covery
<b>CYTOSKELETON</b>							
67483616	EHL_110180	Myosin II heavy chain	247	26	14	40	22
67462785	EHL_159150	Actin	42	10	28	14	38
67468658	EHL_167310	Grainin 2	24	7	22	15	38
67468717	EHL_167300	Grainin 1	24	5	25	8	33
183230870	EHL_155530	Chromosome partition protein	121	3	1,9	2	1,6
103484580	N/A	Clathrin heavy chain	184	2	4,8	8	5
6636336	N/A	Actinin-like protein	63	2	4,8	5	9,7
67478790	EHL_167130	Filopodin	180	2	1,5	5	3,3
67484080	EHL_045000	Actin-related 2/3 complex subunit 1A	40	2	6,6	4	15
67484714	EHL_148890	Calmodulin	17	2	14	4	29
183234431	EHL_120360	Grainin	25	2	12	3	16
67484090	EHL_104630	Filamin 2	95	2	3,5	2	3,2
67477667	EHL_110810	Unconventional myosin IB	119	2	2	2	2,7
<b>PROTEINASES</b>							
183231030	EHL_127030	Peptidase-CP-C6	58	7	12	5	14
67469327	EHL_033710	Cysteine proteinase, CP-A2	35	4	15	6	18
67479681	EHL_136440	Dipeptidyl-peptidase (lipase family)	77	4	4,9	5	15
183231521	EHL_093970	Peptidase-CP-C13	69	4	6,6	3	7,9
67463512	EHL_182720	Dipeptidyl-peptidase ((lipase family)	76	3	6,5	7	11
183231582	EHL_010340	Peptidase-CP-C5	64	3	5,4	3	5,6
67465637	EHL_037190	Serine carboxypeptidase Sp2	54	2	2,7	5	5,2
544088	EHL_074180	Cysteine proteinase, CP-A1	35	2	5,6	4	14
67480901	EHL_152220	Peptidase-CP-C4	58	2	4,6	3	7,4
67469932	EHL_168240	Cysteine proteinase, CP-A5	35	1	5,3	3	7,9

doi:10.1371/journal.pntd.0001002.t002

uropod fractions. The released surface proteins, cytoskeleton-related proteins and cysteine proteases identified herein might help us to understand the mechanism of surface receptor capping and uropod formation. Given that the Gal/GalNAc lectin complex is widely described as being involved in capping [13,14,15], we decided to extend our proteomic analysis by studying the cysteine proteases' roles and M17's localization during uropod formation.

### Inhibition of cysteine proteinases does not change surface receptor capping and uropod formation

Active cysteine proteinases (such as cathepsin X) have been shown to interact with  $\beta$ 2 integrin and to cause cytoskeletal rearrangements that stimulate T lymphocyte migration and uropod formation. Membrane-associated *E. histolytica* cysteine and serine proteases may have a role in the degradation of the tight junctions of target cells, since it has been reported that use of the corresponding inhibitors prevents this process [58,60]. Therefore, we sought to investigate whether or not cysteine proteases present in the UEF have hydrolytic activity and so determined the protease activity of this fraction in a gelatin gel assay (Figure 4A). The data evidenced a good correlation between the patterns generated by peptidases present in the UEF on one hand and the digestion pattern previously published carrying CP-A1, CP-A2 and CP-A5 activities on the other [61]. The data also

corroborated the previous report in which 48, 34 and 17 kDa bands are associated with proteolytic activity and corresponded to CP-A1, CP-A2, and CP-A5, respectively [61]. We thus can infer that active cysteine proteinases were present in the UEF. We confirmed by immunofluorescence the presence of CP-A1, -A2 and -A5 on the uropod of trophozoites incubated with Con A (figure 4C). Interestingly, in addition of the uropod, the antibody detecting both CP-A1 and -A2 stained also at the leading edge of *E. histolytica*, whereas the CP-A5 stained more accurately the membrane surface. In order to investigate the impact of cysteine proteinases in *E. histolytica* uropod formation, we determined the influence of cysteine protease inhibitors on the uropod formation efficiency. Live parasites were incubated in the presence of either cell-permeant E64 (which acts on both extra and intracellular CPs) or cell-impermeant E64 (which acts on extracellular CPs only) at 100  $\mu$ M. The number of uropod-positive cells was not significantly lower in the presence of these inhibitors in three experiments performed. To investigate whether CP-A5 has a specific role in uropod formation, the behaviour of *E. histolytica* silenced for CP-A5 gene expression [20] (i.e. RB8 strain) was examined. Incubation of RB8 parasites and its parental strain G3 with Con A showed that the parasites had equivalent uropod formation rates (two experiments performed). This finding indicated that although cysteine proteinases are abundant and active in the uropod

fraction, they do not influence the dynamics of receptor capping or uropod formation. Cysteine proteinases are important for pathogenicity in *E. histolytica*; given their abundance in the extruded amoebic uropod fractions, we expected them to have much the same functions in surface receptor capping and uropod formation as they do in leukocytes. However, inhibition of cysteine protease activity did not significantly modify the efficiency of cap formation and thus emphasized a contrast with the known role of cysteine peptidases in leukocyte uropod formation.

### Serum from amoebiasis patients induces M17 enrichment at the uropod

Except for the detailed results on the Gal/GalNAc lectin's capping at the amoebic surface and localization of CRT in the uropod, there are no literatures describing other capped surface molecules in *E. histolytica*. One of the major goals of the present work was to identify surface molecules that might have an important role in the development of amoebiasis and/or the onset of immune responses against *E. histolytica*. These objectives prompted us to analyse further M17 in the process of surface receptor capping. We first investigated the domain architecture of M17. This protein was predicted to contain an N-terminal transmembrane domain and a galactose-binding-like domain (Figure 5A). Galactose-binding-like domains (InterPro: IPR008979) are structurally conserved as a beta-sandwich and are responsible for binding to specific ligands, such as cell-surface-attached carbohydrate substrates and phospholipids on the outer face of the mammalian cell membrane. In fact, meta-prediction of the structure of M17's galactose-binding-like domain suggested that its three-dimensional folding is similar to that seen in a number of prokaryotic carbohydrate binding proteins. Indeed, the best hit of this meta-prediction was an extracellular carbohydrate-active virulence factor from *Clostridium perfringens*, GH84C [62]. Sequence alignment of M17 homologues in *Entamoeba* species and GH84C suggests the conservation of three critical carbohydrate-binding residues (Figure 5). Hence, M17 is likely to be located on the cell surface and has a potential role in the carbohydrate-mediated binding of the amoeba to its host cells [63].

In previous work, antibody-antigen caps were induced by incubation of *E. histolytica* with an anti-M17 monoclonal antibody [35]. However, given the absence of control experiments using

unrelated monoclonal antibodies in the initial report, cap formation may have been caused by the mere presence of immunoglobulins (regardless of their specificity) in the antibody fraction. The abundance of M17 in the UEF proteome and its potential role in amoebic physiology prompted us to perform a cellular analysis of M17 during the receptor capping process. We generated a specific anti-M17 antibody for use in western blots and for immunolocalization studies in entire cells. Confocal microscopy analysis clearly demonstrated that M17 localized to the amoebic plasma membrane (Figure 6). To determine the relevance of M17 translocation to the uropod, we looked at whether this protein appeared at the uropod following cell activation with Con A and following incubation of *E. histolytica* with serum from patients with amoebiasis. Staining with the specific anti-M17 antibody and high-resolution confocal microscopy revealed that in both instances, M17 translocated to the rear cell region (Figure 6). Furthermore, at least half of the uropods formed after exposure to sera from patients contained the M17 (two sera were tested). These results clearly showed that M17 is not only on the parasite surface but is also recruited to the uropod following incubation with serum from amoebiasis-positive patients (and not naive sera). The complexity of the uropod protein fraction being discarded to the external medium raises the question for further exploration of the interplay between circulating M17 and other immunodominant antigens in amoebiasis-triggered immune responses.

### Discussion

The uropod is a dynamic structure generated at the rear of polarized mobile cells. It trails the cells and contains various surface proteins. Depending on the nature of the capped surface proteins, a broad panel of biological functions can be associated with this structure. Uropods might be functionally involved in (i) connecting intercellular stalks which facilitate cell-cell interactions in processes such as antigen transport, cytotoxicity, leukocyte extravasation and apoptosis, (ii) providing mechanical forces necessary for motility and cell deformability by facilitating cell passage through constricted spaces and (iii) serving as a site of active bidirectional traffic, in which endocytosis and exocytosis are regulated in a coordinated manner [3]. Furthermore, it has been suggested that *E. histolytica* uses uropods to escape from the host's immune responses; it has been shown that during actomyosin II-based contraction, uropods are released into the external medium and lead to an accumulation of ligand-receptor complexes. In some cases, the ligands (such as antibodies and complement) have anti-amoebic activities. The discarded fraction might also have a role in triggering further steps in the immune response during parasite invasion. Our study showed that sera from amoebiasis patients (but not naive sera) induced a remarkably clustering of molecules in the uropod of *E. histolytica*, suggesting that surface molecule clustering may have a significant impact on the immune response. This finding is critical for future developments in diagnosis and/or vaccination against *E. histolytica*, since the molecules discarded through uropod release circulate in the blood and are very likely to enter into contact with endothelial cells and with immune cells in charge of molecule clearance, antigen presentation and the induction of inflammation.

Here, we have reported that stimulation of *E. histolytica* with the lectin Con A as an experimental model enabled the analysis of the initial capping, then uropod formation and the dynamics of capping in living cells. The engagement of ligand-receptor interactions at the amoebic surface prompted a very rapid change in cell morphology, followed by uropod formation and the

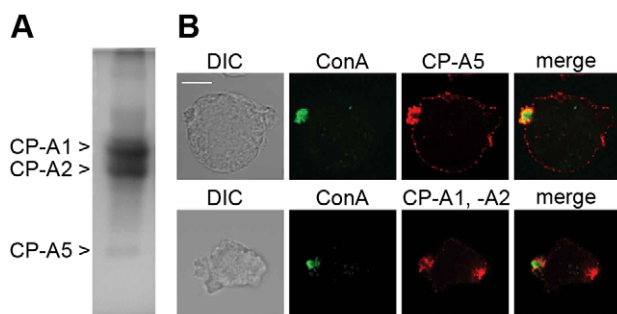


**Figure 4. Cysteine proteinases are present as pro-enzymes and active enzymes in the uropod extruded fractions.** A. Substrate gel electrophoresis of uropod extruded fractions (1  $\mu$ g of proteins), which were separated by electrophoresis in SDS-PAGE co-polymerized with gelatine. To visualize the cysteine proteinase activity, gels were stained with Coomassie blue. The figure shows the inverted image. B. Cellular localisation of CP-A5, -A1 and -A2 in *E. histolytica*. Trophozoites were incubated with Con A (green). Upon incubation, the cells were fixed and stained for CP-A5 (up panel) or CP-A1 and -A2 (low panel) with specific antibodies (red). Scale bar: 10  $\mu$ m. doi:10.1371/journal.pntd.0001002.g004

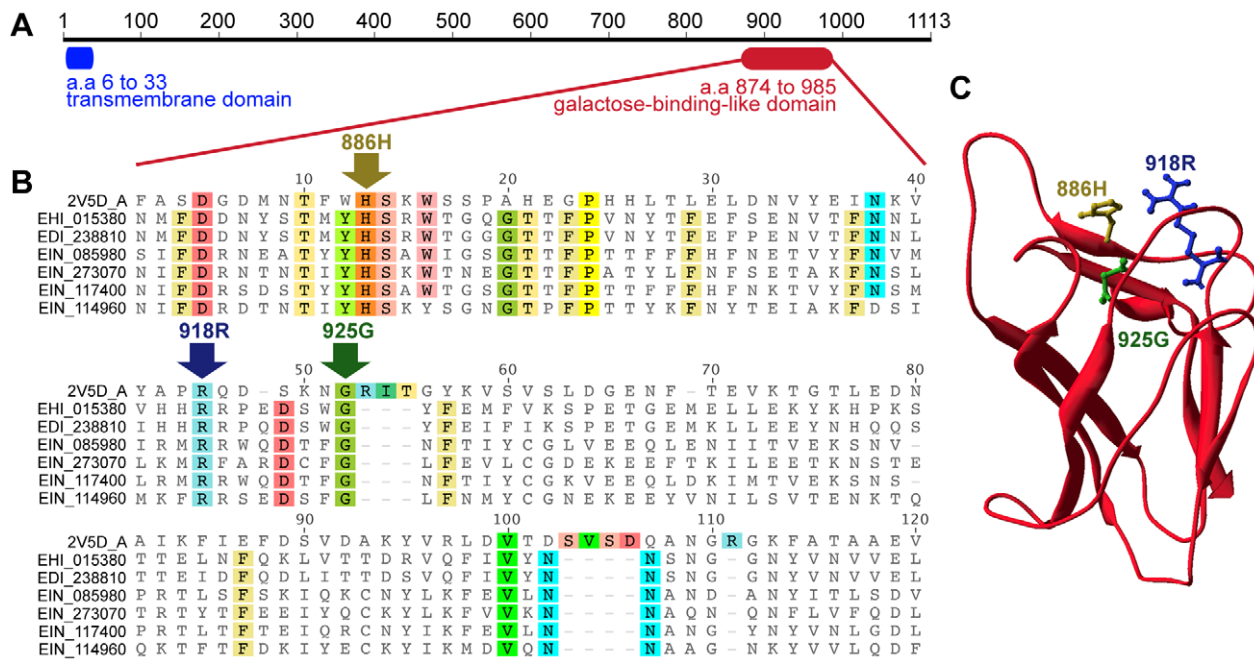


**Figure 5. Conservation of carbohydrate-binding residues in the galactose-binding-like domain of M17 homologues of *Entamoeba*.** A. The domain architecture of M17 (EHI\_015380). The transmembrane domain and the galactose binding-like domain (IPR008979) were identified using Philius [66] and InterProScan software packages, respectively. B. The amino acid sequence alignment of the carbohydrate-binding domain of M17 homologues in *Entamoeba* and GH84C of *C. perfringens* (PBD ID: 2V5D\_A). Residues with >75% identity are highlighted. M17 homologues of *E. dispar* (prefix EDI) and *E. invadens* (prefix EIN) were identified using BLASTP analysis of their proteomes, with M17 as the query. The arrows indicate the carbohydrate binding residues in GH84C [62]. C. Predicted structural model of the galactose-binding like domain of M17. The model was predicted from the 3D jury meta-server [67], with *C. perfringens* GH84C as the best-hit template (i.e. the template with the highest 3D-jury score=81.56; score of 50 is the default cut-off, which results in a prediction accuracy of above 90%). The side-chains of the three conserved carbohydrate binding residues are coloured and labelled as in panel B. doi:10.1371/journal.pntd.0001002.g005

extrusion of membrane fractions. We identified *E. histolytica*'s uropod-associated proteins by performing a proteomic analysis of the released fractions. We determined the presence of disease-relevant surface molecules which are important candidates for the interaction of *E. histolytica* with human cells, including the Gal/GalNAc lectin, CRT, STIRP and ADH112 proteins. Furthermore, we described the clustering of the immunodominant variable antigen M17 - an abundant component of caps formed using either Con A or serum from infected patients. The latter findings indicate that this protein is important for eliciting an immune response. However, genome sequencing has shown that M17-encoding genes also exist in various non-pathogenic *Entamoeba* species (Figure 5). Additional studies will be needed to determine the special features of this antigen in pathogenic species.

We also identified molecules known to regulate actin-based cytoskeleton activities; this revealed a clear difference between uropods in amoebae and those in immune cells. For example, leukocyte uropods contain a microtubule (MT) organizing center. However, the fact that MT disruption in leukocytes does not impair uropod formation suggests that MTs (which are nuclear in *E. histolytica*) are not essential for this process. In contrast, cell polarization and uropod formation in *E. histolytica* are mainly regulated by polymerized actin networks maintained by spectrin-family actin-binding proteins. The latter include  $\alpha$ -actinin and the filamins, which were previously found to accumulate at the uropod and interact with the COOH-terminal domain of the Gal/GalNAc lectin [14]. Our proteomic analysis newly identified an ERM-domain containing protein. In cells, ERM proteins act as membrane-cytoskeleton linkers by interacting with the amino-terminal domains

of membrane proteins and the carboxyl-terminal domain of F-actin [64]. The proteins are pivotal in the signal transduction pathway triggered by receptor capping. For instance, it has been shown [50] that the preferential localization of ezrin (an ERM containing protein) in the uropod of leukocytes requires Thr567 phosphorylation and induces enhancement of uropod integrity, chemotaxis and polar cap formation. Interestingly, some transmembrane adhesion molecules (including CD43, CD44, intercellular adhesion molecules, and PSGL-1) are concentrated at the uropod in immune cells [3] because they have a motif within the intracellular domain which can bind to ERM-containing proteins.

A striking difference between uropods from human cells and those in *E. histolytica* concerns the role of cysteine proteases. In migrating lymphocytes, cathepsin X localizes at the uropod and causes cytoskeletal rearrangements by modulating the activity of  $\beta$ 2-integrin containing receptor LFA-1. The pro-form of cathepsin X carries a RGD motif (also present in CP-A5 from *E. histolytica*) which interacts with the integrin. The protease then cleaves the four last amino acids of the  $\beta$ 2-chain, resulting in its binding to talin - a crucial step in uropod elongation and cell polarization [23]. In contrast, CP-A5 (as well as other CPs) does not have any activity in uropod formation - at least judging by the data obtained with protease inhibitors and the CP-A5-silenced strain. Alternatively, other proteases may have a role in uropod formation, despite the fact that knockdown of the rhomboid serine protease (which specifically localizes at the base of the cap, rather than in the cap itself) had no significant impact on cap formation [65]. The fact that cysteine proteinases from the C family were highly represented in the UEF make these factors relevant for further

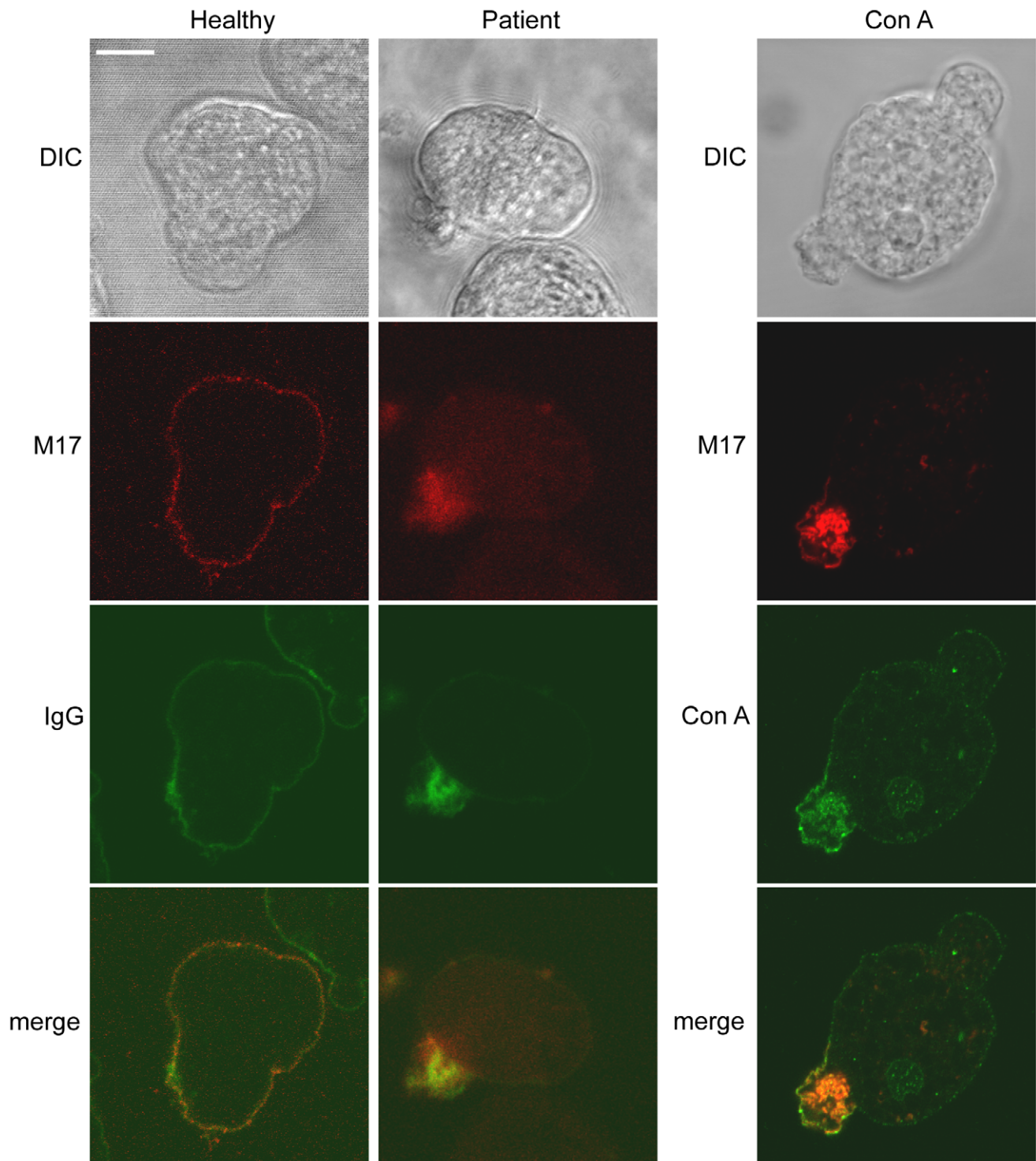


**Figure 6. The cellular localization of the immunodominant antigen M17 in *E. histolytica*.** Trophozoites were incubated with serum from healthy patients (left panels), with serum from patients with amoebic liver abscesses (middle panels) or with green fluorescent Con A (right panels). Upon incubation, the cells were fixed and stained for M17 with a specific antibody (red) and co-stained with a serum recognizing anti-human IgG (left and middle panels). Scale bar: 10  $\mu$ m.  
doi:10.1371/journal.pntd.0001002.g006

analysis. Although cysteine proteases has been found into internal vesicles and/or on the amoebic surface, little is known about the potential association of trafficking vesicles and uropod membranes and/or subcortical cytoskeleton, but we cannot exclude this

possibility. For instance, the pseudopod at the front of the cells is devoid of vesicles. At the moment, we can not confirm these CPs are interacting with the cytoskeleton in *E. histolytica* but it is totally possible, since in leukocytes cathepsin X interacts with the tail of  $\beta$ -

integrin in the cytosol upon activation by cathepsin B in the lysosomes [22]. Hopefully we can get more insight in this point when single cell analysis will be performed trying to determine the dynamics of vesicle traffic in *E. histolytica*.

In conclusion, *E. histolytica*'s trailing edge accumulates important molecules (such as adhesion receptors, immune response activators, cytoskeleton components and proteinases) following the activation of surface receptor capping. In human infection, extrusion of these molecules into the interstitial cell space or the blood can trigger immune responses against *E. histolytica*. These proteins are potentially powerful markers for (i) studying the mechanism underlying uropod formation; (ii) addressing the question of how their activity (or their presence) elicits an immune response and induces cell death when in contact with human cells.

## Supporting Information

**Table S1** Proteins identified at the uropod of *Entamoeba histolytica*. Found at: doi:10.1371/journal.pntd.0001002.s001 (0.05 MB XLS)

**Video S1** Uropod formation in *Entamoeba histolytica*. Trophozoites were seeded on glass bottom culture dishes (MatTeck) and incubated at 37°C in the presence of 5 µg/ml of fluorescent Con A

## References

- Bretscher MS (1996) Getting membrane flow and the cytoskeleton to cooperate in moving cells. *Cell* 87: 601–606.
- Bretscher MS (2008) Recap on cell migration. *Traffic* 9: 198–199.
- Sanchez-Madrid F, Serrador JM (2009) Bringing up the rear: defining the roles of the uropod. *Nat Rev Mol Cell Biol* 10: 353–359.
- Haque R, Huston CD, Hughes M, Houpt E, Petri WA, Jr. (2003) Amebiasis. *N Engl J Med* 348: 1565–1573.
- Santi-Rocca J, Rigother MC, Guillen N (2009) Host-microbe interactions and defense mechanisms in the development of amoebic liver abscesses. *Clin Microbiol Rev* 22: 65–75.
- Calderon J, Avila EE (1986) Antibody-induced caps in *Entamoeba histolytica*: isolation and electrophoretic analysis. *J Infect Dis* 153: 927–932.
- Espinosa-Cantellano M, Chavez B, Calderon J, Martinez-Palomo A (1992) *Entamoeba histolytica*: electrophoretic analysis of isolated caps induced by several ligands. *Arch Med Res* 23: 81–85.
- Petri WA, Jr., Haque R, Mann BJ (2002) The bittersweet interface of parasite and host: lectin-carbohydrate interactions during human invasion by the parasite *Entamoeba histolytica*. *Annu Rev Microbiol* 56: 39–64.
- Abd-Alla MD, Jackson TF, Soong GC, Mazanec M, Ravdin JI (2004) Identification of the *Entamoeba histolytica* galactose-inhibitable lectin epitopes recognized by human immunoglobulin A antibodies following cure of amoebic liver abscess. *Infect Immun* 72: 3974–3980.
- Vines RR, Ramakrishnan G, Rogers JB, Lockhart LA, Mann BJ, et al. (1998) Regulation of adherence and virulence by the *Entamoeba histolytica* lectin cytoplasmic domain, which contains a beta2 integrin motif. *Mol Biol Cell* 9: 2069–2079.
- Cheng XJ, Hughes MA, Huston CD, Loftus B, Gilchrist CA, et al. (2001) Intermediate subunit of the Gal/GalNAc lectin of *Entamoeba histolytica* is a member of a gene family containing multiple CXXC sequence motifs. *Infect Immun* 69: 5892–5898.
- Cheng XJ, Tsukamoto H, Kaneda Y, Tachibana H (1998) Identification of the 150-kDa surface antigen of *Entamoeba histolytica* as a galactose- and N-acetyl-D-galactosamine-inhibitable lectin. *Parasitol Res* 84: 632–639.
- Arhets P, Gounon P, Sansonetti P, Guillen N (1995) Myosin II is involved in capping and uroid formation in the human pathogen *Entamoeba histolytica*. *Infect Immun* 63: 4358–4367.
- Marion S, Tavares P, Arhets P, Guillen N (2004) Signal transduction through the Gal-GalNAc lectin of *Entamoeba histolytica* involves a spectrin-like protein. *Mol Biochem Parasitol* 135: 31–38.
- Tavares P, Rigother MC, Khun H, Roux P, Huerre M, et al. (2005) Roles of cell adhesion and cytoskeleton activity in *Entamoeba histolytica* pathogenesis: a delicate balance. *Infect Immun* 73: 1771–1778.
- Blazquez S, Rigother MC, Huerre M, Guillen N (2007) Initiation of inflammation and cell death during liver abscess formation by *Entamoeba histolytica* depends on activity of the galactose/N-acetyl-D-galactosamine lectin. *Int J Parasitol* 37: 425–433.
- Coudrier E, Amblard F, Zimmer C, Roux P, Olivo-Marin JC, et al. (2005) Myosin II and the Gal-GalNAc lectin play a crucial role in tissue invasion by *Entamoeba histolytica*. *Cell Microbiol* 7: 19–27.
- Bansal D, Ave P, Kerneis S, Frileux P, Boche O, et al. (2009) An ex-vivo human intestinal model to study *Entamoeba histolytica* pathogenesis. *PLoS Negl Trop Dis* 3: e551.
- Blazquez S, Guigon G, Weber C, Syan S, Simeiro O, et al. (2008) Chemotaxis of *Entamoeba histolytica* towards the pro-inflammatory cytokine TNF is based on PI3K signalling, cytoskeleton reorganization and the Galactose/N-acetylgalactosamine lectin activity. *Cell Microbiol* 10: 1676–1686.
- Bracha R, Nuchamowitz Y, Anbar M, Mirelman D (2006) Transcriptional silencing of multiple genes in trophozoites of *Entamoeba histolytica*. *PLoS Pathog* 2: e48.
- Baxt LA, Baker RP, Singh U, Urban S (2008) An *Entamoeba histolytica* rhomboid protease with atypical specificity cleaves a surface lectin involved in phagocytosis and immune evasion. *Genes Dev* 22: 1636–1646.
- Jevnikar Z, Obermajer N, Bogyo M, Kos J (2008) The role of cathepsin X in the migration and invasiveness of T lymphocytes. *J Cell Sci* 121: 2652–2661.
- Jevnikar Z, Obermajer N, Kos J (2009) Cysteine protease-mediated cytoskeleton interactions with LFA-1 promote T-cell morphological changes. *Cell Motil Cytoskeleton* 66: 1030–1040.
- Girard-Misguich F, Sachse M, Santi-Rocca J, Guillen N (2008) The endoplasmic reticulum chaperone calreticulin is recruited to the uropod during capping of surface receptors in *Entamoeba histolytica*. *Mol Biochem Parasitol* 157: 236–240.
- Gonzalez E, Rico G, Mendoza G, Ramos F, Garcia G, et al. (2002) Calreticulin-like molecule in trophozoites of *Entamoeba histolytica* HM1:IMSS (Swissprot: accession P83003). *Am J Trop Med Hyg* 67: 636–639.
- Arhets P, Olivo JC, Gounon P, Sansonetti P, Guillen N (1998) Virulence and functions of myosin II are inhibited by overexpression of light meromyosin in *Entamoeba histolytica*. *Mol Biol Cell* 9: 1537–1547.
- Guillen N, Boquet P, Sansonetti P (1998) The small GTP-binding protein RacG regulates uroid formation in the protozoan parasite *Entamoeba histolytica*. *J Cell Sci* 111: 1729–1739.
- Ghosh S, Samuelson J (1997) Involvement of p21racA, phosphoinositide 3-kinase, and vacuolar ATPase in phagocytosis in bacteria and erythrocytes by *Entamoeba histolytica*: suggestive evidence for coincidental evolution of amoebic invasiveness. *Infect Immun* 65: 4243–4249.
- Aguilar-Rojas A, Almaraz-Barrera Mde J, Krzeminski M, Robles-Flores M, Hernandez-Rivas R, et al. (2005) *Entamoeba histolytica*: inhibition of cellular functions by overexpression of EhGEF1, a novel Rho/Rac guanine nucleotide exchange factor. *Exp Parasitol* 109: 150–162.
- Arias-Romero LE, de la Rosa CH, Almaraz-Barrera Mde J, Diaz-Valencia JD, Sosa-Peinado A, et al. (2007) EhGEF3, a novel Dbl family member, regulates EhRacA activation during chemotaxis and capping in *Entamoeba histolytica*. *Cell Motil Cytoskeleton* 64: 390–404.
- Gonzalez De la Rosa CH, Arias-Romero LE, de Jesus Almaraz-Barrera M, Hernandez-Rivas R, Sosa-Peinado A, et al. (2007) EhGEF2, a Dbl-RhoGEF from *Entamoeba histolytica* has atypical biochemical properties and participates in essential cellular processes. *Mol Biochem Parasitol* 151: 70–80.
- Arias-Romero LE, de Jesus Almaraz-Barrera M, Diaz-Valencia JD, Rojo-Dominguez A, Hernandez-Rivas R, et al. (2006) EhPAK2, a novel p21-activated kinase, is required for collagen invasion and capping in *Entamoeba histolytica*. *Mol Biochem Parasitol* 149: 17–26.
- Labruyere E, Zimmer C, Galy V, Olivo-Marin JC, Guillen N (2003) EhPAK, a member of the p21-activated kinase family, is involved in the control of *Entamoeba histolytica* migration and phagocytosis. *J Cell Sci* 116: 61–71.

34. Vargas M, Sansonetti P, Guillen N (1996) Identification and cellular localization of the actin-binding protein ABP-120 from *Entamoeba histolytica*. *Mol Microbiol* 22: 849–857.
35. Edman U, Meraz MA, Rausser S, Agabian N, Meza I (1990) Characterization of an immuno-dominant variable surface antigen from pathogenic and nonpathogenic *Entamoeba histolytica*. *J Exp Med* 172: 879–888.
36. Orozco E, Lopez C, Gomez C, Perez DG, Marchat L, et al. (2002) Multidrug resistance in the protozoan parasite *Entamoeba histolytica*. *Parasitol Int* 51: 353–359.
37. Diamond LS, Harlow DR, Cunnick CC (1978) A new medium for the axenic cultivation of *Entamoeba histolytica* and other *Entamoeba*. *Trans R Soc Trop Med Hyg* 72: 431–432.
38. Hou Y, Mortimer L, Chadec K (2010) *Entamoeba histolytica* cysteine proteinase 5 binds integrin on colonic cells and stimulates NF $\kappa$ B-mediated pro-inflammatory responses. *J Biol Chem* 285(46): 35497–504.
39. Mitra BN, Saito-Nakano Y, Nakada-Tsukui K, Sato D, Nozaki T (2007) Rab11B small GTPase regulates secretion of cysteine proteases in the enteric protozoan parasite *Entamoeba histolytica*. *Cell Microbiol* 9: 2112–2125.
40. Mai Z, Samuelson J (1998) A new gene family (ariel) encodes asparagine-rich *Entamoeba histolytica* antigens, which resemble the amebic vaccine candidate serine-rich *E. histolytica* protein. *Infect Immun* 66: 353–355.
41. Buss SN, Hamano S, Vidrich A, Evans C, Zhang Y, et al. (2010) Members of the *Entamoeba histolytica* transmembrane kinase family play non-redundant roles in growth and phagocytosis. *Int J Parasitol* 40: 833–843.
42. Tavares P, Sansonetti P, Guillen N (2000) Cell polarization and adhesion in a motile pathogenic protozoan: role and fate of the *Entamoeba histolytica* Gal/GalNAc lectin. *Microbes Infect* 2: 643–649.
43. Garcia-Rivera G, Rodriguez MA, Ocadiz R, Martinez-Lopez MC, Arroyo R, et al. (1999) *Entamoeba histolytica*: a novel cysteine protease and an adhesin form the 112 kDa surface protein. *Mol Microbiol* 33: 556–568.
44. Martinez-Lopez C, Orozco E, Sanchez T, Garcia-Perez RM, Hernandez-Hernandez F, et al. (2004) The EhADH112 recombinant polypeptide inhibits cell destruction and liver abscess formation by *Entamoeba histolytica* trophozoites. *Cell Microbiol* 6: 367–376.
45. Banuelos C, Garcia-Rivera G, Lopez-Reyes I, Orozco E (2005) Functional characterization of EhADH112: an *Entamoeba histolytica* Bro1 domain-containing protein. *Exp Parasitol* 110: 292–297.
46. Pan S, Wang R, Zhou X, Corvera J, Kloc M, et al. (2008) Extracellular Alix regulates integrin-mediated cell adhesions and extracellular matrix assembly. *Embo J* 27: 2077–2090.
47. MacFarlane RC, Singh U (2007) Identification of an *Entamoeba histolytica* serine-, threonine-, and isoleucine-rich protein with roles in adhesion and cytotoxicity. *Eukaryot Cell* 6: 2139–2146.
48. Raz E, Schejter ED, Shilo BZ (1991) Interallelic complementation among DER/flb alleles: implications for the mechanism of signal transduction by receptor-tyrosine kinases. *Genetics* 129: 191–201.
49. Roberts GC, Critchley DR (2009) Structural and biophysical properties of the integrin-associated cytoskeletal protein talin. *Biophys Rev* 1: 61–69.
50. Lee JH, Katakai T, Hara T, Gonda H, Sugai M, et al. (2004) Roles of p-ERM and Rho-ROCK signaling in lymphocyte polarity and uropod formation. *J Cell Biol* 167: 327–337.
51. Wang XY, Ostberg JR, Repasky EA (1999) Effect of fever-like whole-body hyperthermia on lymphocyte spectrin distribution, protein kinase C activity, and uropod formation. *J Immunol* 162: 3378–3387.
52. Blanchoin L, Pollard TD, Mullins RD (2000) Interactions of ADF/cofilin, Arp2/3 complex, capping protein and profilin in remodeling of branched actin filament networks. *Curr Biol* 10: 1273–1282.
53. Clark CG, Alsmark UC, Tazreiter M, Saito-Nakano Y, Ali V, et al. (2007) Structure and content of the *Entamoeba histolytica* genome. *Adv Parasitol* 65: 51–190.
54. Tillack M, Biller L, Irmer H, Freitas M, Gomes MA, et al. (2007) The *Entamoeba histolytica* genome: primary structure and expression of proteolytic enzymes. *BMC Genomics* 8: 170.
55. Jacobs T, Bruchhaus I, Dandekar T, Tannich E, Leippe M (1998) Isolation and molecular characterization of a surface-bound proteinase of *Entamoeba histolytica*. *Mol Microbiol* 27: 269–276.
56. Ankri S, Stolarsky T, Bracha R, Padilla-Vaca F, Mirelman D (1999) Antisense inhibition of expression of cysteine proteinases affects *Entamoeba histolytica*-induced formation of liver abscess in hamsters. *Infect Immun* 67: 421–422.
57. Lechner AM, Assfalg-Machleidt I, Zahler S, Stoeckelhuber M, Machleidt W, et al. (2006) RGD-dependent binding of procathepsin X to integrin  $\alpha$ 5 $\beta$ 3 mediates cell-adhesive properties. *J Biol Chem* 281: 39588–39597.
58. Barrios-Ceballos MP, Martinez-Gallardo NA, Anaya-Velazquez F, Mirelman D, Padilla-Vaca F (2005) A novel protease from *Entamoeba histolytica* homologous to members of the family S28 of serine proteases. *Exp Parasitol* 110: 270–275.
59. JWong H, Schotz MC (2002) The lipase gene family. *Lipid Res* 43: 993–9.
60. Lauwaet T, Oliveira MJ, Callewaert B, De Bruyne G, Mareel M, et al. (2004) Proteinase inhibitors TPCK and TLCK prevent *Entamoeba histolytica* induced disturbance of tight junctions and microvilli in enteric cell layers *in vitro*. *Int J Parasitol* 34: 785–794.
61. Irmer H, Tillack M, Biller L, Handal G, Leippe M, et al. (2009) Major cysteine peptidases of *Entamoeba histolytica* are required for aggregation and digestion of erythrocytes but are dispensable for phagocytosis and cytopathogenicity. *Mol Microbiol* 72: 658–667.
62. Ficko-Blean E, Gregg KJ, Adams JJ, Hehemann JH, Czjzek M, et al. (2009) Portrait of an enzyme, a complete structural analysis of a multimodular  $\beta$ -N-acetylglucosaminidase from *Clostridium perfringens*. *J Biol Chem* 284: 9876–9884.
63. Marion S, Guillen N (2006) Genomic and proteomic approaches highlight phagocytosis of living and apoptotic human cells by the parasite *Entamoeba histolytica*. *Int J Parasitol* 36: 131–139.
64. Fehon RG, McClatchey AI, Bretscher A (2010) Organizing the cell cortex: the role of ERM proteins. *Nat Rev Mol Cell Biol* 11: 276–287.
65. Baxt LA, Rastew E, Bracha R, Mirelman D, Singh U (2010) Downregulation of an *Entamoeba histolytica* rhomboid protease reveals roles in regulating parasite adhesion and phagocytosis. *Eukaryot Cell* 9(8): 1283–93.
66. Reynolds SM, Kall L, Riffle ME, Bilmes JA, Noble WS (2008) Transmembrane topology and signal peptide prediction using dynamic bayesian networks. *PLoS Comput Biol* 4: e1000213.
67. Ginalski K, Elofsson A, Fischer D, Rychlewski L (2003) 3D-Jury: a simple approach to improve protein structure predictions. *Bioinformatics* 19: 1015–1018.